14th European Signal Processing Conference (EUSIPCO 2006), Florence, Italy, September 4-8, 2006, copyright by EURASIP

ADAPTIVE SUBBAND NOTCH FILTER FOR RFI CANCELLATION IN LOW INTERFERENCE TO SIGNAL RATIO

[1,2]Rim Elasmi-Ksibi, [1]Sofiane Cherif, [1]Hichem Besbes and [2]Mériem Jaïdane

(1) Unité de Recherche TECHTRA, SUPCOM, Tunisia
(2) Unité de Recherche Signaux et Systèmes, ENIT, Tunisia
{asmi.rim, sofiane.cherif, hichem.besbes}@supcom.rnu.tn, meriem.jaidane@enit.rnu.tn

ABSTRACT

In this paper, an adaptive-subband-based Radio Frequency Interference (RFI) cancellation method for VDSL systems is developed. The use of subband adaptive IIR notch filter with a specific developed excision algorithm offers a solution in low Interference to Signal Ratio (ISR) environment. The division of a fullband problem into several subbands improves the tracking ability of the Fullband Adaptive Notch Filter (FANF) in low ISR, since the noise variance is reduced in each subband and offers faster convergence speed, due to decimation. In this paper, we compare the performances of the subband method with the classical fullband method using the normalized-stochastic-algorithm-based IIR Adaptive Notch Filter (ANF).

1. INTRODUCTION

VDSL system is a promising technology that provides fast data connection (up to 52 Mbps). As the VDSL transmission bandwidth is extended between 1.1 to 30 Mhz, a VDSL receiver has to face Radio Frequency Interference (RFI) from Amplitude Modulation (AM) radio stations, Short Wave (SW) radio stations and mainly amateur SW radio. The RFI is considered as the main disturbance source that can be damaging to VDSL receiver. The power density level of the RFI signal depends on the interference distance to the VDSL receiver.

As the RFI signal band is narrow with respect to the VDSL receiver spectrum, the RFI signal can be modeled as a sum of sinusoids and the VDSL signal as a noise. An adaptive RFI suppressor should converge fast to the incident frequency and for different levels of power density of the RFI signal. Usually, adaptive IIR notch filter can be used as an adaptive RFI suppressor (see for example [1], [2], [3]).

The high accuracy of the sine wave frequency estimates is important to guarantee that the narrow notches will cancel the input sine wave. A statistical analysis, done in [4], shows that the accuracy of the sine wave is associated with the choice of the filter bandwidth and the Interference to Signal Ratio (ISR). The narrower the bandwidth and the larger the ISR, the smaller the distortion in the wide band component of the filter is achieved.

The proposed structures of adaptive IIR notch filters exploit the fullband of the observed signal. The performances of these structures are extremely limited for low ISRs ([1], [2]). This has motivated the use of Subband Adaptive Notch Filter (SANF).

The advantage of subband adaptive filter is due to decimation since the M times longer sampling period increases the convergence rate of the applied algorithm with respect to the fullband case. Others advantages of this structure include the reduction of noise variance, as the subbands have reduced bandwidth than the fullband. On top of that, computationally efficient and memory-saving implementations for the subband splitting can be achieved through modulated filters [5].

In the following, section 2 presents the fullband system model. In section 3, we introduce the adaptive subband IIR notch filter. Then, a technique based on threshold is introduced to detect the branch which contains the sinusoidal component. Simulation results confirm that the proposed structure converges faster and gives better performances for low ISR compared to Fullband Adaptive Notch Filter (FANF).

2. POOR PERFORMANCES OF FULLBAND SYSTEM FOR LOW ISR

This paper deals with the detection of one source of RFI. Since, the RFI can be modeled as a sine wave, we will be interested in the estimation of the unknown frequency w_0, of a pure sine wave $s(n)$, immersed in a noise $u(n)$:

$$\begin{aligned} y(n) &= s(n)+u(n) \\ &= \alpha\sin(w_0 n+\varphi)+u(n), \end{aligned} \tag{1}$$

where α is the amplitude of the sinusoid, φ is its random phase and $u(n)$ is an additive noise which is assumed to be independent of $s(n)$.

Usually, 2^{nd} order IIR filters with constrained parameterizations are used as a structure in a notch-based-estimation technique. The structure, presented by [4], is typically used in practice. It has the following expression :

$$\begin{aligned} H(z) &= \frac{1+a(n)z^{-1}+z^{-2}}{1+a(n)rz^{-1}+r^2z^{-2}} \\ &= \frac{A\left(z^{-1}\right)}{A\left(rz^{-1}\right)}, \end{aligned} \tag{2}$$

where $A(z)=1+a(n)z+z^2$, $a(n)=-2\cos w(n)$, $w(n)$is the frequency estimate and the parameter r $(0\leq r<1)$ is known as the pole contraction factor.

The basic idea underlying notch-filters-based estimation techniques is the minimization, with respect to $a(n)$, of the Mean Square Error (MSE) of the notch filter output $e(n)$, fed by the observation signal $y(n)$. It leads to minimize the cost function :

$$J(n)=E\left(e^2(n)\right). \tag{3}$$

To adjust the filter coefficient $a(n)$ of the above notch filter form, we will use the normalized stochastic algorithm (NLMS). The update equations, considered in this paper are given by :

$$a(n+1) = a(n) - \frac{\mu}{\beta(n)} e(n)\psi(n), \quad (4)$$

$$\beta(n+1) = \lambda(n)\beta(n) + |\psi(n)|^2; \quad (5)$$

where μ is the step size, $\lambda(n)$ is a varying forgetting factor and $\psi(n)$ is the differential of $e(n)$ with respect to $a(n)$ and is referred to as the gradient error estimation.
Most of the existing implementations of the ANF deal with the fullband implementation (see references cited therein). It has been shown that the accuracy of the minimum-mean-square-error based ANF depends on two parameters : the interference to signal ratio (ISR) and the pole contraction factor r of the notch filter [2].
The influence of the ISR on the accuracy of the frequency estimate, when the pole contraction factor is chosen close to 1, is presented in the following.
The input sine wave has unit magnitude and is corrupted by zero-mean white gaussian noise. The frequency of the input sinusoid, w_0, was 0.15. Since r and $\lambda(n)$ affect the convergence speed of the algorithm, we apply the algorithm with small values for r and $\lambda(n)$ at the beginning of the algorithm's operation and increase their values later. Therefore, an exponential function is often used. In these simulations, the values of r and $\lambda(n)$ are set varying from 0.9 to 0.995.
Table 1 presents the variance of the estimated frequency for different ISRs. In this simulation, we have done 100 independent experiments for signals with various ISRs.
As can be seen from this table, when ISR= 5 dB, the FANF performs well. When $ISR = 0$ dB, the variance of the estimated frequency increases, so the tracking performance of the algorithm reduces. Morever, some realizations have outlier performances, due to local instability of the adaptive IIR fullband notch filter. The experiment is considered as outlier occurring if the frequency estimate is not close to the typical behavior. As expected, the number of outliers increases significantly for low ISRs, since the condition of instability situation increases.

Table1 : FANF simulation results of 100 independent experiments for sine wave in additive white noise.

ISR (dB)	FANF
5	8.7462×10^{-9}
0	0.0649
-5	0.83
-10	1.2691

Employing subband decomposition, we outperform the conventional frequency domain of fullband system. Since the input signal is decomposed into several subbands, the noise variance is reduced and so, we get a higer ISR level. In this paper, we introduce an alternative notch-based-estimation technique employing subband decomposition to improve the algorithm performance to track the desired frequency for low ISR level.

3. FILTER BANK FOR RFI CANCELLATION

3.1 Design of adaptive subband IIR notch filter

Filter bank is used to divide the received signal into several subbands (analysis part). The input signal $y(n)$ is split into M subbands, using an adequate analysis filters, decimated and then an adaptive notch filter is used in each band to estimate the desired frequency. The interference detector presented in this paper is based on a Modulated Filter Bank (MFB). This structure has emerged as an optimum filter bank with respect to implementation cost and design ease since only the prototype filter is designed ([5], [6], [7], etc...).
Figure 1 shows the block diagram of the proposed SANF for the RFI cancellation. Let $F_k(z)$ the transfer function of the analysis filter in the k^{th} subband where $0 \leq k \leq M-1$. We note $y_k(n)$, the filtered and downsampled version of the original signal $y(n)$ and $L_k(z)$, the adaptive IIR notch filter in subband k, attempting to minimize the subband error signal $e_k(n)$ in this branch. The expression of $L_k(z)$ is :

$$L_k(z) = \frac{A_k\left(z^{-1}\right)}{A_k\left(rz^{-1}\right)}, \quad 0 \leq k \leq M-1; \quad (6)$$

where $A_k(z) = 1 + a_k(n)z + z^2$; $a_k(n) = -2\cos w_k(n)$ is the adjusted coefficient in branch k and w_k is the unknown frequency in this branch.

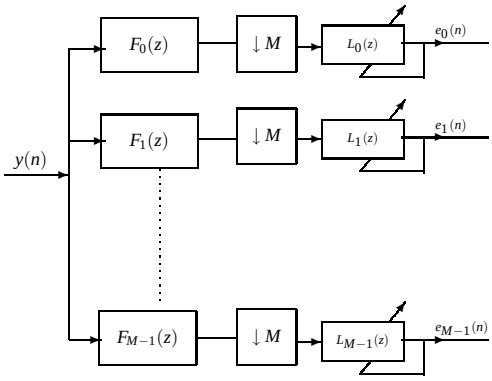

Figure 1: Multi-band implementation of the adaptive IIR notch filter.

To explain the principle of interference detection, we will consider a two-subband filter bank that can be extended to the multi-band scheme.
In our scheme of RFI cancellation, we must identify the branch which contains the sine wave and reject the other branch from our schema of suppression.

3.2 The excision principle

The detection of the sinusoid is based on thresholds. A simple effective way is to measure the powers of the subbands, at the input $P_y^k = E(y_k^2(n))$ and at the output of the adaptive notch filter $P_e^k = E(e_k^2(n))$, where $k = 0,1$ designs the subband number.
The subband with lower output-power to input-power ratio $\rho_k = \frac{P_e^k}{P_y^k}$ contains the sinusoidal term and in this case the sine wave frequency estimate is given by the adjusted coefficient

$a_k(n)$ of the filter $L_k(z)$. Due to decimation, the filter coefficient estimate $\hat{a}(n)$ is related to the parameter estimate in each branch as follows :

$$\hat{a}(n) = \begin{cases} \sqrt{2-a_0(n)} & \text{if } \rho_0 \leq \theta \text{ and } \rho_1 > \theta \\ -\sqrt{2-a_1(n)} & \text{if } \rho_1 \leq \theta \text{ and } \rho_0 > \theta \end{cases}, \quad (7)$$

where θ is the threshold.
To fix the threshold θ, we will express the signal power at the output of the notch filter P_e^k. It is easy to see that P_e^k can be calculated as follows :

$$P_e^k = E\left(e_k^2(n)\right) = \frac{1}{2\pi j}\oint L_k(z)L_k(z^{-1})S_y^k(z)z^{-1}dz, \quad (8)$$

where $S_y^k(z)$ is the power spectrum of $y_k(n)$. If $y_k(n)$ contains the sine wave, it can be split into the power spectra of $s_k(n)$, the sinusoidal component and $u_k(n)$, the noise, namely: $S_y^k(z) = S_s^k(z) + S_u^k(z)$.
We consider a white noise with variance σ_u^2 and the random phase of the sine wave is uniformly distributed in the interval $[0, 2\pi[$. Thanks to equtions (8) and (6), we have :

$$P_e^k = E_s^k(w_k) + E_u^k(w_k). \quad (9)$$

The expressions of $E_s^k(w_k)$ and $E_u^k(w_k)$ are (see appendix A):

$$E_s^k(w_k) = 2\alpha^2 \frac{(\cos(w_0) - \cos(w_k))^2}{h(w_k, w_0, r)}, \quad (10)$$

where

$$h(w_k, w_0, r) = \left(1-r^2\right)^2 - 4r(1+r^2)\cos(w_k)\cos(w_0) + 4r^2\left(\cos^2(w_k) + \cos^2(w_0)\right)$$

and

$$E_u^k(w_k) = \sigma_u^2 \frac{-2(3r-1)\cos^2 w_k + (1+r)\left(1+r^2\right)}{(r+1)\left[\left(1+r^2\right)^2 - 4r^2\cos^2 w_k\right]}. \quad (11)$$

Three cases that allow as to specify the threshold can occur.
a) **First case**: A sinusoid exists in the branch k and it is detected by the SANF. In these conditions, we have :

$$\begin{cases} P_y^k = \frac{\alpha^2}{2} + \frac{\sigma_u^2}{2} \\ P_e^k \simeq E_u^k(w_0) \end{cases}. \quad (12)$$

b) **Second case**: A sinusoid exists in the branch k and it is'nt detected by the SANF. In these conditions, we have :

$$\begin{cases} P_y^k = \frac{\alpha^2}{2} + \frac{\sigma_u^2}{2}, \\ P_e^k = E_s^k(w_k) + E_u^k(w_k) \quad \text{with} \quad w_k \neq w_0. \end{cases} \quad (13)$$

c) **Third case**: A sinusoid does'nt exist in the branch k. In these conditions, we have :

$$\begin{cases} P_y^k = \frac{\sigma_u^2}{2}, \\ P_e^k = E_u^k(w_k) \quad \text{with} \quad w_k \neq w_0. \end{cases} \quad (14)$$

It is important to note that the shape of ρ_k in these three cases induces the adequate threshold.

The figure 2 plots the shape of $2E_u^k(w_k)/\sigma_u^2$ in the ranges of $w_k \in [0, \pi]$ and $r \in [0, 0.999]$, which corresponds to ρ_k for the third case.
The figure 3 plots the shape of ρ_k, for the first case and the second case, in the ranges of $w_k \in [0, \pi]$, and for different ISR levels.
Let $g(w_k, w_0, r) = (E_s^k(w_k) + E_u^k(w_k))/(\frac{\alpha^2}{2} + \frac{\sigma_u^2}{2})$. From figure 3, we note that $g(w_k, w_0, r)$ is minimum and its value is always less to 1 for the correct detection $w = w_0$. When the sinusoid is not detected, w_k a value far from the frequency w_0, we note that the value of $g(w_k, w_0, r)$ is greater than 1. So, a threshold $\theta = 1$ can be chosen, when the contraction pole is too close to 1.

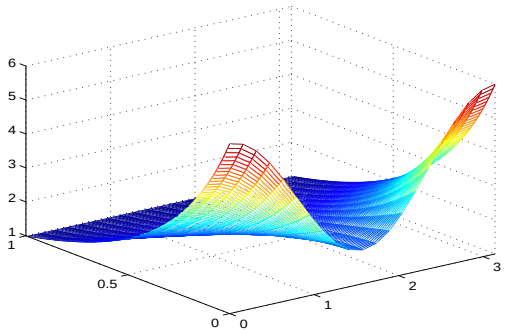

Figure 2: Shape of the function $2E_u^{k)}(w_k)/\sigma_u^2$ in the ranges $w_k \in [0, \pi]$ and $r \in [0, 0.999]$.

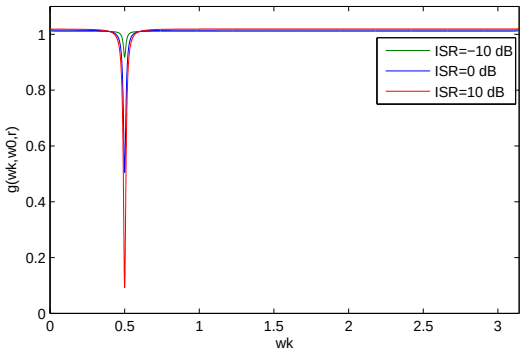

Figure 3: Shape of the function $g(w_k, w_0, r)$ in the range $w_k \in [0, \pi]$, $r = 0.99$, $w_0 = 0.5$.

4. PERFORMANCE COMPARISON

Two simulations are analysed in order to compare SANF and FANF performances.
In the first experiment, we consider the same simulation conditions as introduced above. We present a table that summarizes the resulting variance statistics of the sine wave frequency estimate. We have tried 100 independent experiments using SANF for different subband numbers.
From Table 1 and Table 2, we observe that SANF has nearly identical tracking performances as the FANF when ISR=5

dB. For low ISR, inferior to 0 dB, while FANF fail to obtain correct frequency estimate, the SANF reduces the number of failed cases and improves the tracking performances of the fullband adaptive notch filter. The ability of the algorithm to track the desired frequency increases with the number of subbands. For example, when the number of bands is equal to 16, the SANF converges accurately to the correct estimate in all the experiences for ISR=-5 dB (variance=3.5311×10^{-9}).

Table2 : SANF simulation results of 100 independent experiments for sine wave in additive white noise.

ISR dB	SANF (M=2)	SANF (M=4)	SANF (M=16)
5	8.2944×10^{-10}	3.1933×10^{-10}	1.4146×10^{-10}
0	0.0036	8.361×10^{-9}	2.4231×10^{-10}
-5	0.076	0.0057	3.5311×10^{-9}
-10	0.8018	0.5429	0.1949

In the second simulation, we compare the convergence speed of SANF and FANF. The ISR is equal to 5 dB. We consider the same signal as in last simulations.
The frequency estimation of FANF and SANF is showed in figure 4. The convergence of the SANF is faster than the FANF. Indeed, to achieve a frequency estimate that deviates from the truth frequency by 0.01, FANF needs 850 iterations while the SANF (M=2) converges at 250 iterations and SANF (M=16) converges at 50 iterations.

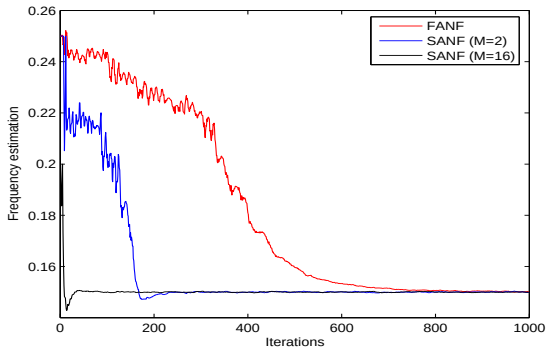

Figure 4: Frequency estimation of FANF and SANF (M=2, M=16), ISR=5 dB.

5. CONCLUSION

We have presented a subband implementation of adaptive IIR notch filter algorithm. This scheme has faster convergence rate and the high accuracy of the sine wave frequency estimate for low ISR than the fullband case. This result is obtained due to an adequate choice of the threshold.
It is interesting to generalize this analysis for colored noise and for input signal consisting of a finite number of sinusoids.

Appendix A

We use residue calculations to establish the expressions of $E_s^k(w_k)$ and $E_u^k(w_k)$ (equations (10) and (11)).

$$\begin{aligned} E_s^k(w_k) &= \frac{1}{2\pi j}\oint L_k(z)L_k(z^{-1})S_s^k(z)z^{-1}dz \\ &= \frac{\alpha^2}{2}\mathrm{Re}\left|L_k\left(e^{jw_0}\right)\right|^2 \\ &= 2\alpha^2\frac{\left(\cos(w_0)-\cos(w_k)\right)^2}{h(w_k,w_0,r)}, \end{aligned}$$

where

$$\begin{aligned} h(w_k,w_0,r) &= \left(1-r^2\right)^2 - 4r(1+r^2)\cos(w_k)\cos(w_0) + \\ &\quad 4r^2\left(\cos^2(w_k)+\cos^2(w_0)\right) \end{aligned}$$

and

$$\begin{aligned} E_u^k(w_k) &= \frac{\sigma_u^2}{4\pi j}\oint L_k(z)L_k(z^{-1})S_u^k(z)z^{-1}dz \\ &= \frac{\sigma_u^2}{4\pi j}\oint \frac{A_k(z)}{z\left(z^2A_k\left(rz^{-1}\right)\right)}\frac{A_k(z)}{A_k(rz)}dz \quad r<z<\frac{1}{r} \\ &= \sigma_u^2\frac{-2(3r-1)\cos^2 w_k + (1+r)\left(1+r^2\right)}{(r+1)\left[\left(1+r^2\right)^2 - 4r^2\cos^2 w_k\right]}. \end{aligned}$$

REFERENCES

[1] M. H. Cheng and J. L. Tsai, "A new adaptive notch filter with constrained poles and zeros using steiglitz-mcbride method," *IEEE International Symposium on circuits and systems-ICASSP98*, pp. 1469–1472, May 1998.

[2] A. Nehorai, "A minimal parameter adaptive notch filter with constrained poles and zeros," *IEEE transactions on acoustics, speech and signal processing*, vol. ASSP-33, no. 4, pp. 983–996, 1985.

[3] Y. L. P. S. Diniz and T. I. Laakso, "Adaptive steiglitz mc bride notch filter design for radio interference suppression in vdsl systems," *in Proc. IEEE Globecom-2001*, 2001.

[4] A. Nehorai, "Performance analysis of an adaptive notch filter with constrained poles and zeros," *IEEE transactions on acoustics, speech and signal processing*, vol. 36, no. 6, pp. 911–919, 1988.

[5] T. A. Ramstad and J. P. Tanem, "Cosine-modulated analysis-synthesis filter bank with critical sampling and perfect reconstruction," *IEEE Int. Conf. ASSP (Toronto)*, vol. ASSP-37, pp. 1789–1792, 1991.

[6] J. Mau, "Perfect-reconstruction modulated filter banks," *IEEE Conf. ASSP*, 1992.

[7] J.Princen and A. Bradley, "Analysis/synthesis filter bank design based on time domain aliasing cancellation," *IEEE Trans. Acoust. Speech Signal Processing*, pp. 1153–1161, 1986.